Presented at the 15th ICFA Advanced Beam Dynamics Workshop on Quantum Aspects of Beam Physics, January 4-9, 1998.

QUANTUM FLUCTUATIONS IN BEAM DYNAMICS

KWANG-JE KIM
Accelerator Systems Division, Advanced Photon Source
Argonne National Laboratory
9700 South Cass Avenue, Argonne, IL 60439
E-mail: kwangje@aps.anl.gov

Quantum effects could become important for particle and photon beams used in high-luminosity and high brightness applications in the current and next generation accelerators and radiation sources. This paper is a review of some of these effects.

1 Introduction

The main aim of modern particle accelerators for high energy physics is to produce high energy particle beams and collide them with a high luminosity:

$$\mathcal{L} = f_c \frac{N^2}{4\pi\sigma_x^*\sigma_y^*} \tag{1}$$

where f_c is the collision frequency, N is the number of particles in each bunch, and $\sigma_x^*(\sigma_y^*)$ is the rms beam size at the collision point in the x (y) direction. Similarly, the main aim of modern synchrotron radiation facilities is to produce x-ray photons with high brightness:

$$\mathcal{B} = \alpha \frac{f_b N}{(2\pi)^2 \varepsilon_x \varepsilon_y} \tag{2}$$

where α is the fine structure constant, f_b is the bunch repetition frequency, and $\varepsilon_x(\varepsilon_y)$ is the rms emittance in the x (y) direction. If the radiation source is at the symmetry point of a straight section, as is usually the case, the emittance is given by

$$\varepsilon_x = \sigma_x \sigma_{x'}, \quad \varepsilon_y = \sigma_y \sigma_{y'}. \tag{3}$$

where $\sigma_x(\sigma_y)$ and $\sigma_{x'}(\sigma_{y'})$ are, respectively, the rms beam size and angular divergence in the x (y) direction. (In Eq. (2), we have neglected the radiation phase space area compared to the particle phase space area—a good approximation for x-ray photons.)

The requirement of either high luminosity for particle collision or high brightness for radiation production leads to the requirement of small emittance. This is evident for a high-brightness radiation source in view of Eq. (2). It is also true for high luminosity because of the practical limit on angular divergence to achieve a small spot size σ_x^*.

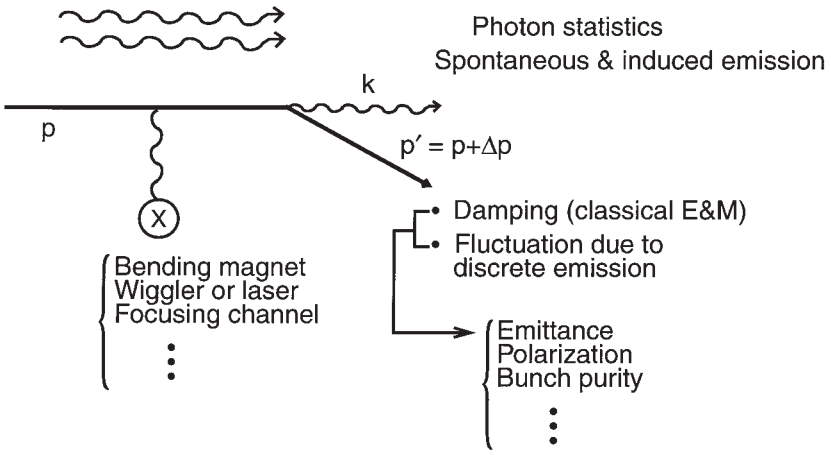

Figure 1: Schematic illustration of various quantum effects in particle and photon beams and their interaction.

Quantum mechanical effects become important in the dynamics of extremely high-brightness beams because the beam becomes sensitive to quantum recoils and also because of possible wavefunction degeneracy. Various quantum effects in the interaction of high-brightness particle and radiation beams are schematically summarized in Fig. 1. This paper contains discussions of some of these topics.

Section 2 gives a review of basic phase-space constraints due to quantum mechanics. Section 3 is a review of a well-understood topic, the quantum fluctuation in storage rings, from the view that the synchrotron radiation is a manifestation of the Hawking-Unruh radiation. The approach provides a fresh look at the equilibrium emittance (section 3.2) and polarization in electron storage rings (section 3.3). Section 4 deals with the quantum effects in free-electron lasers (FELs). A simple discussion of the gain reduction due to the quantum recoil is given in section 4.1. Quantum effects are also important for photon statistics and start-up noise in self-amplified spontaneous radiation, which is the subject of section 4.2.

Max Zolotorev played an important role in preparation of this paper, especially for the material in section 3. He derived Eq. (15), which is the basis of the rest of section 3.2, and was available for extensive discussions during the development of section 3.4 and other parts of the paper.

This paper can be regarded as an incomplete summary of the discussions

that took place in Working Group A. Some of the interesting and important topics discussed are not included here, including the spin polarization in electron and proton beams by D. Barber, quantum chaos probed by rf cavities by F. Zimmerman, and bunch diffusion in electron storage rings by J. Byrd.

2 Wave Functions and Phase-Space Distribution of Quantum Particles

In quantum mechanics, a particle in free space behaves as a wave packet [1]. The wave number for $\gamma \gg 1$ is given by

$$q = \frac{\gamma}{\lambda\!\!\!^{-}_c},$$

where $\lambda\!\!\!^{-}_c$ is the Compton wavelength $= \hbar/mc$, which, for an electron, is 3.8×10^{-13} m. The Heisenberg uncertainty principle can be written as

$$\varepsilon_x^n \geq \lambda\!\!\!^{-}_c/2, \quad \varepsilon_y^n \geq \lambda\!\!\!^{-}_c/2, \quad \varepsilon_z^n \geq \lambda\!\!\!^{-}_c/2. \tag{4}$$

Here ε_i^n are the normalized emittances:

$$\varepsilon_x^{(n)} = \gamma\varepsilon_x, \quad \varepsilon_y^{(n)} = \gamma\varepsilon_y, \quad \varepsilon_z^{(n)} = \sigma_z\sigma_\gamma, \tag{5}$$

where the transverse emittances are given by Eq. (3), and in longitudinal emittance ε_z^n, σ_z is the rms packet length, and σ_γ is the rms value of $\gamma - \gamma_0$, where γ_0 is the nominal energy.

Equation (4) can be interpreted as the fact that the phase-space area occupied by a quantum particle cannot be smaller than $\lambda\!\!\!^{-}_c/2$. The equality holds for a Gaussian wave packet.

There is some ambiguity in assigning the relative magnitudes of classical beam emittance and the single-particle, quantum emittance. The ambiguity can be removed by introducing the emittance based on the entropy concept, as was done for the classical wave optics [2].

The concept of phase space for a quantum mechanical particle can be based on the Wigner distribution [3]. Although the Wigner distribution cannot be assigned to a real probability distribution because it could be negative locally, it is nevertheless useful because of its similarity to the real probability distribution of classical particles in phase space. Thus the transformation properties of the quantum phase-space distribution as the particle travels through free space and quadrupole focusing elements, etc., are identical to those in classical particle distribution as illustrated in Figure 2. Through a free space, the quantum phase-space distribution is tilted along the x-axis exactly as in the

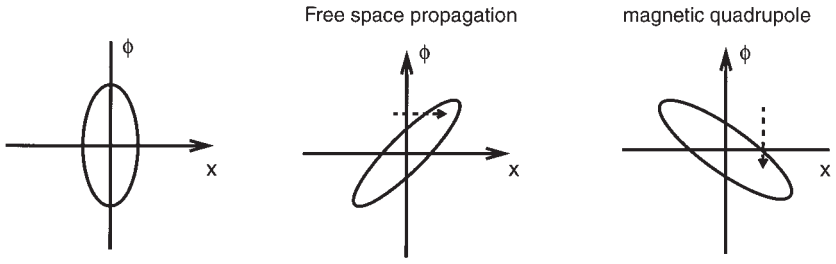

Figure 2: Phase-space representation of a quantum particle and its behavior while passing through some accelerator elements.

case of a classical distribution. Similarly, it is tilted down the x'-axis through a focusing element, again, exactly as in the classical distribution.

A collection of quantum particles are described by a collection of wave packets centered along the classical particle trajectories as shown in Figure 3. The phase-space distribution is then a convolution of the classical beam distribution and the quantum mechanical distribution of a single particle, as shown in Figure 4. The total phase-space area is minimal when the phase-space ellipses of the classical and the quantum distributions are similar and have the same orientation, i.e., when they are *matched*. Once matched, they remain matched because the transformation properties of the classical and quantum phase space are the same, as mentioned before.

The total phase-space volume of an N-particle beam is limited by the statistics. For Fermions we have

$$\varepsilon_x^{(n)}\varepsilon_y^{(n)}\varepsilon_z^{(n)} \geq N(\lambda\!\!\!^{-}_c/2)^3/(2S+1), \tag{6}$$

where S is the spin. For Bosons, on the other hand, the limit is given by

$$\varepsilon_x^{(n)}\varepsilon_y^{(n)}\varepsilon_z^{(n)} \geq (\lambda\!\!\!^{-}_c/2)^3. \tag{7}$$

Equations (6) and (7) give the degeneracy limits. Close to these limits, quantum mechanical effects will become important.

The collection of quantum mechanical wave packets discussed here is similar to the optical wave packets generated by a charged particle beam, such as the synchrotron radiation beam. The synchrotron radiation beam optics based on the Wigner distribution was discussed earlier[4].

The identity of the transformation properties between the quantum mechanical (or optical) phase space and the classical phase space via the Wigner

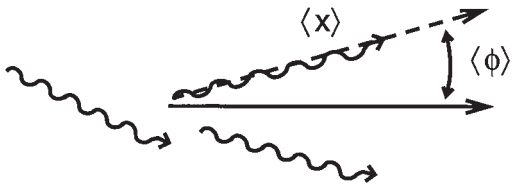

Figure 3: Quantum beam as a collection of wave packets (wavy lines) each of which is centered along a classical trajectory (dotted lines).

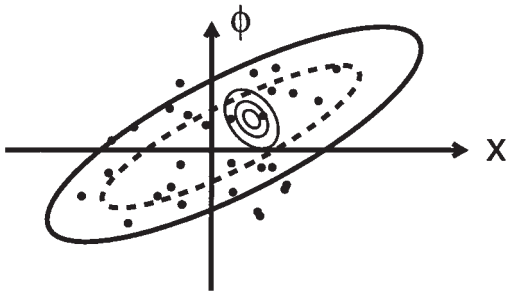

Figure 4: Total phase space of a quantum beam (solid ellipse) as a convolution of the single-particle quantum phase space (represented by small concentric ellipses) and the classical beam phase space (dotted ellipse).

distribution is valid for linear transport elements such as free space and ideal quadrupoles. In the presence of aberrations, the equivalence needs to be modified [5].

3 Understanding the Quantum Fluctuations in Electron Storage Rings

In electron storage rings the equilibrium beam emittance is determined by the balance of the damping effect due to the classical synchrotron radiation and the quantum fluctuation due to the discreteness of the photon emission process. This is a well-understood topic [6,7]. During the workshops, the nature of Hawking-Unruh radiation was the subject of extensive debate. Here we adopt the point of view that Hawking-Unruh radiation is simply another description of the well-known synchrotron radiation. With this point of view, it is possible to develop a "simple" understanding of the equilibrium beam parameters in storage rings.

The main goal of this section is to provide a new physical understanding of well-understood phenomenon. Therefore we are interested in the parametric relationships and order of magnitude, and will not be careful about numerical factors of 2π, etc. in this section.

3.1 The Hawking-Unruh Picture

Following up on the celebrated observation by Hawking [8] that a black hole is also a black body radiator, Unruh [9] found that an accelerated particle finds itself being in contact with a heat bath of temperature T given by

$$k_B T = \frac{\hbar a}{2\pi c}, \tag{8}$$

where k_B is the Boltzman constant, $\hbar$ is the Planck constant, a is the acceleration, and c is the speed of light.

For an electron moving on a circular trajectory of radius ρ in a magnetic field, the acceleration is $a = \gamma^2 c^2/\rho$. Therefore, it sees a black body distribution of photons with characteristic frequency ω_c' (the prime represents quantities in the instantaneous rest frame) given by

$$\hbar\omega_c' \simeq k_B T = \frac{\hbar\gamma^2 c}{2\pi\rho}. \tag{9}$$

These photons, which appear to be real to the accelerated electron, are clearly not real in the laboratory frame. However, they can be scattered by the electron to become real photons in the laboratory frame with the well-known

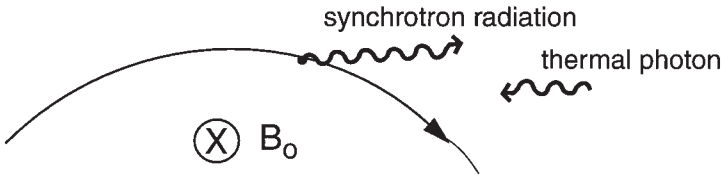

Figure 5: The Hawking-Unruh picture of synchrotron radiation. An accelerating charge finds itself surrounded by thermal photons, which can be scattered by the electron to appear as the real photons of synchrotron radiation.

synchrotron radiation characteristic frequency of $\hbar\omega_c \simeq \hbar\gamma\omega_c' \simeq \hbar\gamma^3 c/\rho$, with a characteristic angular opening γ^{-1}. This is illustrated in Fig. 5.

To develop the picture further, let us consider the radiated power. In a black body distribution, there is on average about one photon per mode occupying a mode volume λ'^3, where λ' is the wavelength. Thus, the scattered power is

$$P_s \simeq \sigma \frac{\hbar\omega_c'}{\lambda'^3} c, \tag{10}$$

where σ is the cross section. On the other hand, the synchrotron radiation power is given by Larmor's formula,

$$P_s = \frac{2}{3} e^2 \frac{a^2}{c^3} = \frac{2}{3} \alpha \hbar \omega_c'^2. \tag{11}$$

Equations (10) and (11) become equal if

$$\sigma = \alpha \lambda'^2. \tag{12}$$

This result may surprise some readers. For atoms with bound electrons, it is well known that the scattering cross section at resonance is λ'^2. The case of Hawking radiation by a black hole is also similar, where λ' is give by r_g, the horizon radius. Equation (12) can be interpreted as the statement that a free electron can only "hold" α photons per mode, rather than one photon per mode in the atomic case.

We emphasize that the Hawking-Unruh picture developed in the above is a particular picture for understanding the synchrotron radiation process from a different perspective. There are other perhaps more familiar pictures. Thus the synchrotron radiation process can be viewed as the "shedding" of Weiszäcker-Williams photons as the electron bends in the magnetic field. It can also be viewed as the scattering of virtual photons contained in the bending magnetic

field. In this case, however, the scattering cross section should be taken as a Thomson cross section.

The Hawking-Unruh picture is well suited for a simple understanding of equilibrium electron beam parameters in storage rings, as we will discuss now.

3.2 Simple Understanding of Equilibrium Electron Distribution in Storage Rings

Consider first the equilibrium energy distribution. Since the accelerating electrons are in equilibrium with a heat bath with temperature given by Eq. (8), the equilibrium kinetic energy in the beam frame must be

$$\langle \Delta E' \rangle = \left\langle \frac{p'^2}{2m} \right\rangle = \frac{3}{2} k_B T \simeq \hbar \gamma^2 c/\rho. \tag{13}$$

On the other hand, the energy spread in the laboratory frame $\Delta E'$ is related to the energy spread $\Delta E'$ in the beam rest frame via

$$\left\langle \left(\frac{\Delta E}{E} \right)^2 \right\rangle = 2 \left\langle \frac{\Delta E'}{mc^2} \right\rangle. \tag{14}$$

Inserting Eq. (14) into Eq. (13), one obtains

$$\left\langle \left(\frac{\Delta E}{E} \right)^2 \right\rangle \simeq \lambda\!\!\!^{-}_c \frac{\gamma^2}{\rho}, \tag{15}$$

reproducing the well-known result [7] up to a factor of order unity. Equation (15) was derived by M. Zolotorev during the workshop.

Next, consider the fluctuation of the betatron oscillation. In the y-direction (vertical to the orbit plane) the electron angular divergence is given by

$$\langle \psi^2 \rangle = \left\langle \left(\frac{p_y}{p_z} \right)^2 \right\rangle = \frac{2m}{p_z^2} \left\langle \frac{p_y^2}{2m} \right\rangle = \frac{2m}{p_z^2} \frac{k_B T}{2}. \tag{16}$$

Therefore, the equilibrium normalized emittance becomes

$$\varepsilon_y^n = \gamma \lambda\!\!\!^{-}_\beta \langle \psi^2 \rangle \simeq \lambda\!\!\!^{-}_c \left(\frac{\lambda\!\!\!^{-}_\beta \gamma}{\rho} \right), \tag{17}$$

where $\lambda\!\!\!^{-}_\beta$ is the betatron wavelength divided by 2π. This is another well-known result.

Equation (17) is valid because the dispersion vanishes in the vertical direction. In the x-direction (the horizontal direction), however, the dispersion effect dominates. In that case we use Eq. (15),

$$\langle (\delta x)^2 \rangle = \eta^2 \left\langle \left(\frac{\Delta E}{E} \right)^2 \right\rangle = \eta^2 \lambda\!\!\!^{-}_c \frac{\gamma^2}{\rho}, \tag{18}$$

where η is the horizontal dispersion $\eta = \lambda\!\!\!^{-2}_\beta / \rho$. Therefore

$$\varepsilon_x^n = \gamma \frac{1}{\lambda\!\!\!^{-}_\beta} \langle (\delta x)^2 \rangle \simeq \lambda\!\!\!^{-}_c \left(\frac{\lambda\!\!\!^{-}_\beta \gamma}{\rho} \right)^3. \tag{19}$$

Again this agrees qualitatively with the well-known result.

3.3 Suppression of Quantum Fluctuation

For most electron storage rings the quantity $\lambda\!\!\!^{-}_\beta \gamma / \rho$ is much larger than unity. This has two consequences: first, the horizontal emittance given by Eq. (19) is much larger than the vertical emittance given by Eq. (17), and second, the vertical emittance is much larger than $\lambda\!\!\!^{-}_c$.

However, if one considers an ideal limit $\rho \to \infty$, with γ and $\lambda\!\!\!^{-}_\beta$ fixed, then the equilibrium emittance would vanish according to Eqs. (17) and (19). In this *straight focusing channel* the emittance does not vanish strictly but is limited by the ultimate emittance given by Eqs. (6) or (7) according to whether the particles are Fermions or Bosons. This case has been analyzed using quantum mechanics [10]. However, the straight focusing channel appears to be difficult to implement because the required length of the channel is too long to be practical.

On the other hand, it is not necessary to have a straight channel. All that is necessary to achieve the ultimate emittance is

$$\chi = \frac{\rho/\gamma}{\lambda\!\!\!^{-}_\beta} \geq 1. \tag{20}$$

Huang et al. [11] have carried out a quantum mechanical analysis of the so-called *bent focusing system* and found that the quantum fluctuation becomes exponentially suppressed as χ becomes larger than 1, leading to the ultimate emittance. It remains to be seen whether a practical storage ring design will emerge from this idea.

3.4 Understanding the Equilibrium Polarization in Electron Storage Rings

An elementary particle has the magnetic dipole moment

$$\mu = g\frac{e\hbar}{2mc}\mathbf{S}, \tag{21}$$

where $\mathbf{S}$ is the spin vector and g is a dimensionless constant that is very close to 2 for electrons. Thus the two spin states of an electron, $S_z = \pm 1/2$, will split in energy under the external magnetic field $\mathbf{B}'_o = \gamma B_o \mathbf{e}_z$. The level spacing is given by

$$\Delta E = g\frac{e\hbar}{2mc}\gamma B_o \simeq g\hbar\omega'_c. \tag{22}$$

Electrons in the upper state would make transitions to the lower state. The electrons from this argument are expected to become 100% polarized after a sufficient time.

This is of course not completely true. It is known that the maximum degree of polarization in an electron storage ring is given by [12]

$$P = \frac{8}{5\sqrt{3}} = 0.924. \tag{23}$$

A lucid discussion of the success as well as the failure of the simple model based on spin splitting and a discussion of a more accurate semiclassical calculation can be found in Jackson [13].

The fact that the degree of polarization is not 100% can be understood easily by the Hawking-Unruh picture [14]. The limiting polarization in this case would be

$$P = \frac{1 - e^{-\Delta E/k_B T}}{1 + e^{-\Delta E/k_B T}} \simeq \frac{1 - e^{-\pi g}}{1 + e^{-\pi g}}. \tag{24}$$

Although Eq. (24) predicts numerically a higher degree of polarization than Eq. (23), it nevertheless provides qualitative understanding on why the polarization is not pure.

It is perhaps instructive to see in more detail how the polarization evolves. Figure 6 shows the two electron energy levels under an external DC magnetic field $\mathbf{B}_0$. The spin flip is caused by the black body photons that are polarized so that the oscillating magnetic field is perpendicular to $\mathbf{B}_0$. If the photon energy is resonant with the level spacing, $\hbar\omega = \Delta E$, spin flip occurs due to the same phenomena as in nuclear magnetic resonance. In the presence of average photon number $\langle n\rangle = \exp(-\hbar\omega/k_B T)$, the up-transition rate is proportional to $\langle n\rangle$, while the down-transition rate is proportional to $\langle n\rangle + 1$. The equilibrium

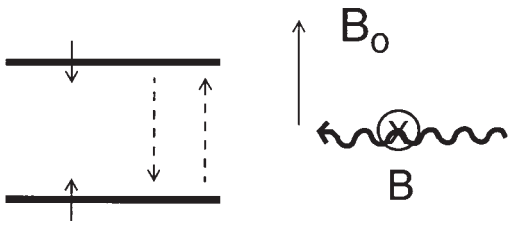

Figure 6: Illustration of electron energy levels in the external magnetic field and the spin flip due to the perturbation by the oscillating magnetic field B (perpendicular to B_o) from the apparent thermal photons.

polarization is therefore

$$P = \frac{\langle n\rangle + 1 - \langle n\rangle}{1 + 2\langle n\rangle} = \frac{1}{1 + 2\langle n\rangle} \simeq \frac{1 - \langle n\rangle}{1 + \langle n\rangle}. \tag{25}$$

This reduces to Eq. (24).

4 Quantum Effects on Free-Electron Lasers

It is well known that the quantum mechanical correction on the classical gain formula becomes important when the photon energy is comparable to, or larger than, the gain bandwidth. A less explored topic is the role of quantum mechanics in the statistics of FEL photons, especially the self-amplified spontaneous emission.

4.1 Quantum Recoil and FEL Gain

The processes of emission and absoption of a photon in the presence of $n-$ photons are schematically illustrated in Fig. 7. The spontaneous emission probability as a function of frequency ω is peaked at the resonance frequency ω_R and can be written as $W_s(\omega - \omega_R)$. The total emission probability W_e is given by [15]

$$W_e = (n+1)W_s(\omega - \omega_e). \tag{26}$$

Here the term proportional to n is due to the induced emission, and ω_e is the resonant emission frequency taking into account the recoil effect:

$$\omega_e = \omega_0 \left(1 - \frac{\hbar\omega_0}{E_e}\right), \tag{27}$$

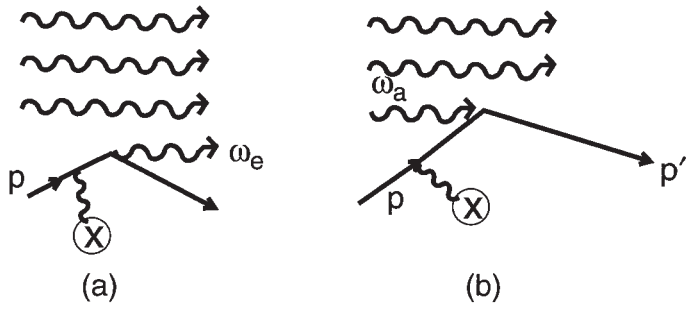

Figure 7: Photon emission (a) and absorption (b) in the presense of n-photons.

where ω_0 is the resonance frequency neglecting the recoil effect, and E_e is the electron energy. Similarly, the total absorption probability is

$$W_a = nW_s(\omega - \omega_a), \tag{28}$$

where

$$\omega_a = \omega_0 \left(1 + \frac{\hbar\omega_0}{E_e}\right) \tag{29}$$

is the resonant absorption frequency.

Thus the net emission probability is

$$\Delta W = W_e - W_a = W_s(\omega - \omega_e) + n[W_s(\omega - \omega_e) - W_s(\omega - \omega_a)]. \tag{30}$$

Neglecting the first term in the RHS of Eq. (30) (the spontaneous emission term) for the case $n \gg 1$, the gain is given by

$$G = \frac{\Delta W}{n} = W_s(\omega - \omega_e) - W_s(\omega - \omega_a). \tag{31}$$

Consider now the case of the stimulated emission process in an undulator, as in the case of the usual free-electron laser. The bandwidth of the spontaneous undulator emission is

$$\frac{\Delta\omega}{\omega_0} \leq \frac{1}{N_u}, \tag{32}$$

where N_u is the number of undulator periods. Therefore, when

$$\frac{\hbar\omega_0}{E_e/N_u} \ll 1, \tag{33}$$

the gain can be expressed as a frequency-derivative of the spontaneous emission spectrum. This form of the classical gain is known as Madey's theorem [16]. On the other hand, when

$$\frac{\hbar\omega_0}{E_e/N_u} \geq 1, \tag{34}$$

then the quantum recoil is significant, and the gain is reduced from the classical case [17,18].

From the inequality of Eq. (34), one sees that the quantum recoil is important for short wavelength FELs based on low-energy electron beam, such as the x-ray FEL using extreme high-brightness e-beam based on field emission from microtips [19].

4.2 Self-Amplified-Spontaneous Emission

The self-amplified spontaneous emission (SASE) is receiving much attention recently as a promising next generation light source for intense, quasi-coherent x-rays. Classical analysis of SASE has been extensively developed in the areas of exponential growth [20] and start-up from the electron shot noise [21,22]. Under a certain set of assumptions, including Eq. (33), it was shown that the evolution of the quantum Heisenberg operator closely parallels that of the classical case [23]. Thus, the field amplitude operator is given by

$$a(\tau) = f_1(\tau)a(0) + f_2(\tau)\Theta(0) + f_3(\tau)P(0), \tag{35}$$

where τ is the normalized time, fs are functions that grow exponentially in τ, and

$$\Theta = \sum_i e^{-i\theta_i}, \quad P = \sum_i p_i e^{-i\theta_i}. \tag{36}$$

In the above, the sum is over all the electrons, and θ_i and p_i are, respectively, the phase and momentum operators for the i^{th} electron ($[\theta_i, p_i] = i$).

The first terms gives rise to the coherent state with Glauber statistics. The second and third terms are due to the electrons' shot noise.

When

$$\varepsilon_x^n \varepsilon_y^n \varepsilon_z^n \gg N\left(\lambda\!\!\!^{-}_c/2\right)^3/2, \tag{37}$$

then Θ and P can be regarded as classical stochastic variables. In this case, the evolution and statistics of the SASE field are those given by the classical analysis. On the other hand, if

$$\varepsilon_x^n \varepsilon_y^n \varepsilon_z^n \leq N\left(\lambda\!\!\!^{-}_c/2\right)^3/2, \tag{38}$$

then the degeneracy of the quantum wave function needs to be taken into account. Thus the wavefunction of the N-Fermion system must be written as

$$|\psi\rangle = \sum_P \frac{(-1)^P}{\sqrt{N!}} |\psi_\alpha(z_1)\rangle |\psi_\beta(z_2)\rangle \ldots \quad |\psi_\gamma(z_n)\rangle, \tag{39}$$

where $\psi_\alpha(z)$ is the one-particle wavefunction, and the sum is over all permutation of $\{z_1, \ldots, z_n\}$ (for Bosons, $(-1)^P \to 1$).

A rigorous analysis of SASE, taking into account the wave function degeneracy appears quite complicated. However, an understanding of the effect can be seen as follows: The effective start-up noise of SASE intensity is proportional to

$$\langle\psi| \Big| \sum_{j=1}^{N} e^{ikz_j} \Big|^2 |\psi\rangle = N + N(N+1) \overline{\langle\psi| e^{ik(z_1 - z_2)} |\psi\rangle}. \tag{40}$$

The first term in the above corresponds to the classical noise. In the second term, the bar denotes averaging over particles. When the inequality Eq. (37) is valid, the second term can be calculated with classical averaging and is negligible when the bunch length is longer than the radiation wavelength. On the other hand, when the inequality Eq. (38) is valid, a proper quantum calculation with suitably anti-symmetrized wavefunction, Eq. (39), is necessary. In the simple case $N = 2$, this can be carried out explicitly, with the result

$$\langle\psi| e^{ik(z_1 - z_2)} |\psi\rangle \simeq \frac{e^{-\sigma_z^2 k^2} \mp e^{-\varepsilon_z^n / \lambda\!\!\!^{-}_c}}{1 \mp e^{-\varepsilon_z^n / \lambda\!\!\!^{-}_c}}. \tag{41}$$

Here the upper (lower) sign corresponds to the Fermion (Boson) case. This reduces to the classical result when $\epsilon_z^n \gg \lambda\!\!\!^{-}_c$. For $\epsilon_z^n \leq \lambda\!\!\!^{-}_c$, the noise is the reduced (increased) in the case of the Ferimionic (Bosonic) system.

Note added in proof.—After the manuscript was completed, it came to the author's attention by Z. Huang that results equivalent to Eqs. (15), (17), and (19) were derived in 1997 by K. McDonald ("The Hawking-Unruh Temperature and Quantum Fluctuations in Particle Accelerators," proceedings of 1997 Particle Accelerator Conference). Also, in 1986 J.S. Bell and J. M. Leinaas ("The Unruh Effect and Quantum Fluctuations of Electrons in Storage Rings," CERN TH 4468-86) derived a result equivalent to Eq. (17) for a weakly focused storage ring.

Acknowledgments

I am grateful to the members of Working Group A of the Workshop on Quantum Aspects of Beam Physics held in Monterey, CA, January 4-9, 1998; to

Max Zolotorev for many discussions and, in particular, for his contribution to the materials in section 3; to Pisin Chen, without whose insistence this paper would not have been written; and to Z. Huang for pointing out both the spin factor in the RHS of Eq. (6) and MacDonald's work.

This work is supported by the U.S. Department of Energy, Office of Basic Energy Sciences, under Contract No. W-31-109-ENG-38.

References

1. See for example, D. Bohm, *Quantum Theory*, Prentice Hall, New York (1951).
2. K.-J. Kim and R.G. Littlejohn, "Entropy and Emittance of Particle and Photon Beam," Proc. of 1995 Part. Accel. Conf., Dallas, TX, 174 (1996).
3. E. Wigner, *Phys. Rev.* **40**, 749 (1932).
4. K.-J. Kim, *Nucl. Instr. Meth.* **A246**, 71 (1986).
5. A.J. Dragt, "Lie algebraic methods for ray and wave optics," proceedings.
6. K. Robinson, *Phys. Rev.* **111**, 373 (1958).
7. See for a review, M. Sands, "The Physics of Electron Storage Rings," SLAC-121 (1970).
8. S.W. Hawking, *Nature* **248**, 30 (1974).
9. W.G. Unruh, *Phys. Rev.*, **D14**, 870 (1976).
10. Z. Huang, P. Chen, and R. D. Ruth, *Phys. Rev. Lett.* **74**, 1759 (1995).
11. Z. Huang and R. D. Ruth, *Phys. Rev. Lett.* **80**, 2318 (1998).
12. A.A. Sokolov and I.M. Ternov, Dokl. Akad. Nauk. SSSR **153**, 1052, 1963 Sov. Phys.-Dokl.8, 1023 (1964).
13. J.D. Jackson, *Reviews of Mod. Physics* **48**, 417 (1976).
14. J.S. Bell and J.M. Leinaas, *Nucl. Phys.* **B212**, 131 (1983).
15. See for example, R. Loudon, *The Quantum Theory of Light*, Clarendon Press, Oxford (1973).
16. J.M.J. Madey, *Nuovo Cim.* **50B**, 64 (1979).
17. J.-Gea-Banacloche, *Phys. Rev.* **A31**, 1607 (1985).
18. See for a review, G. Dattoli and A. Renieri, in *Laser Handbook*, Vol. 6, North-Holland (1990).
19. C. Brau, in proceedings of 1997 FEL Conference (to be published).
20. R. Bonifacio, C. Pelligrini, and L.M. Narducci, *Opt. Commun.* **50**, 373 (1984).
21. K.-J. Kim, *Phys. Rev. Lett.* **57**, 1871 (1988).
22. J.M. Wang and L.H. Yu, Nucl. *Instr. Meth.* A250, 484 (1986).
23. R. Bonifacio and F. Casagrande, *Opt. Commun.* **50**, 251 (1984).